Original Article

A PRECLINICAL ASSESSMENT OF RAPIDLY ISOLATED CHONDRO-PROGENITOR CELLS FROM THE INFRAPATELLAR FAT PAD FOR SINGLE-STAGE ARTICULAR CARTILAGE REGENERATION

D.C. Browe[1,2,3,4], O.R. Mahon[1,2,3,5], P.J. Díaz-Payno[1,2], R. Burdis[1,2], F.E. Freeman[1,2,3,6,7,8], J.M. Nulty[1,2], P. Pitacco[1,2], G. Gonnella[1,2], A. Dunne[3,5], C.J. Moran[1,9,10], P.A.J. Brama[11], C.T. Buckley[1,2,3] and D.J. Kelly[1,2,3,*]

[1]Trinity Centre for Biomedical Engineering, Trinity Biomedical Sciences Institute, Trinity College Dublin, D02 R590 Dublin, Ireland
[2]Department of Mechanical, Manufacturing and Biomedical Engineering, School of Engineering, Trinity College Dublin, D02 PN40 Dublin, Ireland
[3]Advanced Materials and Bioengineering Research Centre (AMBER), Royal College of Surgeons in Ireland and Trinity College Dublin, D02 W9K7 Dublin, Ireland
[4]Altach Biomedical Limited, D04 C5Y6 Dublin, Ireland
[5]School of Biochemistry and Immunology, School of Medicine, Trinity Biomedical Sciences Institute, Trinity College Dublin, D02 R590 Dublin, Ireland
[6]School of Mechanical and Materials Engineering, Engineering and Materials Science Centre, University College Dublin, D04 V1W8 Dublin, Ireland
[7]UCD Centre for Biomedical Engineering, University College Dublin, D04 V1W8 Dublin, Ireland
[8]Conway Institute of Biomolecular and Biomedical Research, University College Dublin, D04 V1W8 Dublin, Ireland
[9]Orthopaedics and Sports Medicine, School of Medicine, Trinity College Dublin, D02 PN40 Dublin, Ireland
[10]Sports Surgery Clinic, D09 C523 Dublin, Ireland
[11]School of Veterinary Medicine, University College Dublin, D04 V1W8 Dublin, Ireland

Abstract

Background: Clinically approved cell-based cartilage repair products are associated with multiple surgeries and high cost. There is therefore an unmet clinical need for a cell-based approach that is efficacious and cost effective that can be performed intraoperatively as a single-stage procedure. **Methods:** Here, we developed a novel methodology to rapidly isolate chondro-progenitor cells from human infrapatellar fat pad tissue that reduced the isolation time from over three hours to under one hour while still being able to yield clinically relevant cell numbers. Cell yields and biochemical characteristics were compared with conventionally isolated control cells. *In vitro* assays evaluated cartilage-specific matrix deposition across multiple human donors. Constructs combining rapidly isolated cells and articular cartilage extracellular matrix-derived scaffolds were implanted into caprine cartilage defects and analyzed after six months *in vivo*. **Results:** These rapidly isolated cells contained a larger fraction of colony-forming cells than conventionally isolated control cells, and an analysis of surface marker expression revealed a higher percentage of $CD44^{+}$ (a putative progenitor cell marker) cells in this group. Furthermore, these rapidly isolated cells supported higher levels of cartilage-specific matrix deposition *in vitro* for multiple human donors. We then seeded such rapidly isolated cells onto cartilage extracellular matrix (ECM) derived scaffolds and immediately (i.e., no *in vitro* pre-culture) implanted these constructs into caprine cartilage defects. After 6 months *in vivo*, treatment with this cell and scaffold combination typically generated a repair tissue that was rich in glycosaminoglycans and type II collagen, with biomimetic collagen fiber alignment and lubricin expression in the superficial zone, which was generally not observed in defects treated with microfracture. However, in this model the addition of the rapidly isolated cells did not result in any significant improvement in repair metrics compared to treatment with the extracellular matrix scaffold alone. **Conclusions:** While this rapidly isolated cell population processes a strong chondrogenic potential *in vitro*, further work is required to identify clinical scenarios where it will provide clear therapeutic benefits.

Keywords: Cartilage repair, articular cartilage, stem cell therapy, tissue engineering, regenerative medicine, biomaterials.

***Address for correspondence**: D.J. Kelly, Trinity Centre for Biomedical Engineering, Trinity Biomedical Sciences Institute, Trinity College Dublin, D02 R590 Dublin, Ireland. Email: kellyd9@tcd.ie.

Introduction

The successful treatment of articular cartilage (AC) injuries remains a key clinical challenge for orthopaedic surgeons [1]. AC has a limited intrinsic repair capacity post-trauma and therefore surgical intervention is necessary to induce repair. Despite over thirty years of advances in cartilage repair procedures, chondroplasty (cartilage debridement), with or without additional bone marrow stimulation techniques such as microfracture (MFX) remains the first line treatment choice for many orthopaedic surgeons due to its low price-point and short surgical time [1,2]. However, the repair tissue generated as a result of MFX generally consists of mechanically inferior fibrocartilage [2–5]. In addition, MFX treatment also reduces the success of subsequent cell-based treatments such as autologous chondrocyte implantation (ACI) or matrix-assisted autologous chondrocyte implantation (MACI) [6,7]. The high cost of cell-based approaches and challenges with reimbursement has hampered their wide-spread clinical use [8]. This has motivated the development of single-stage, cell-based cartilage repair products (e.g., CartiOne^{TM}) that obviates the need for *ex vivo* expansion of autologous chondrocytes by rapidly isolating chondrocytes at the point of care [9]. However, with such products, a biopsy of cartilage from a non-load bearing region must be obtained from the patient, which is far from ideal as donor site morbidity remains a concern [10,11], and these approaches typically require the rapidly isolated chondrocytes to be combined with a bone marrow biopsy or allogenic bone marrow-derived stromal cells (BMSCs) [12–14]. Therefore, there is an unmet clinical need for the development of a cost effective, single-stage, intraoperative (or "in-theatre") cartilage repair therapy that has a short duration of surgery, alleviates any potential concern regarding donor site morbidity, and results in hyaline cartilage-like repair tissue.

The anatomical location of the infrapatellar fat pad (IFP) in the knee joint and the high proportion of putative progenitor cells with chondrogenic potential found in this tissue make the IFP an attractive cell source for cartilage repair applications [15]. Culture expanded infrapatellar fat pad stromal cells (FPSCs) have been demonstrated to have at least comparable chondrogenic capacity to bone marrow-derived stromal cells (BMSCs) and can maintain their chondrogenic capacity in a diseased state [16–19]. More recent research has shown that the IFP is a significant source of perivascular stem cells that possess potent chondrogenic potential [20]. While methodologies for the rapid isolation of stromal cells from IFP and adipose tissue have been described [21], some studies are unclear whether clinically relevant numbers of chondro-progenitors cells can be isolated from the IFP within timeframes compatible with single-stage cartilage repair procedures [22,23]. For example, incubation with collagenase for 60 minutes (with no agitation) yielded between 7.88×10^4 and 67.79×10^4 cells per gram of IFP tissue from multiple donors, which is likely not a sufficient number of cells for clinical use [24]. A more recent study was able to demonstrate that comparable numbers of cells could be rapidly isolated from IFP tissue (in 85 minutes) when compared to a conventional procedure, however these rapidly isolated cells did not demonstrate any improved chondrogenic potential and the rapid isolation procedure employed the use of Matrigel as an attachment substrate which is not approved for human clinical use which is a limitation for clinical translation [25]. Furthermore, the regenerative capacity of such rapidly isolated stromal cells has yet to be assessed in clinically relevant large animal models of AC repair.

The overall goal of this study was to develop a novel methodology to rapidly (less than one hour) isolate chondro-progenitor cells from IFP tissue that could subsequently be used as a cell source for single-stage AC repair procedures. The specific aims of this study were to: (1) Develop a rapid isolation procedure capable of simply and quickly isolating clinically relevant numbers of FPSCs from human IFP tissue. (2) Characterise the phenotype of the rapidly isolated cells in comparison to conventionally isolated FPSCs by examination of the colony forming unit (CFU) potential and cell surface marker expression of cells retrieved using both isolation procedures. (3) Compare the *in vitro* chondrogenic potential of both rapidly and conventionally isolated FPSCs when seeded on previously optimized articular cartilage extracellular matrix (AC-ECM)-derived biomaterial scaffolds. (4) Assess the efficacy of rapidly isolated FPSCs, when seeded onto AC-ECM scaffolds, as a single-stage AC repair therapy in a clinically relevant, large animal study. We chose to combine these rapidly isolated stromal cells with AC-ECM derived scaffolds as this biomaterial has previously been shown to support robust chondrogenic differentiation of culture expanded human FPSCs [26,27]. In addition, these AC-ECM derived scaffolds have been shown to promote endogenous cartilage repair without the inclusion of cells in both chondral [28] and osteochondral defects [29] in large animal models.

Materials and Methods

Infrapatellar Fat Pad (IFP) Tissue Harvest

IFP tissue was obtained from patients undergoing total knee replacement surgery (mean age 55 years ± 2 years) (Donor A = male 55 years old, Donor B = male 53, Donor C = female 57 years old). No details except the age and sex of the donors were provided. For flow cytometry experiments, IFP biopsies were harvested from non-diseased patients undergoing anterior cruciate ligament (ACL) reconstruction surgery. All four donors were male (mean age 22.25 years ± 3.8 years). Between 0.5 g and 1 g of IFP tissue was harvested per donor. Once the tissue was excised, it was transferred to a sterile container, placed on ice and immediately

transported to the laboratory for immediate cell isolation. The time from tissue harvest to commencing the isolation procedure was between 45–60 minutes.

Fat Pad Stromal Cell (FPSC) Isolation Procedure

IFP tissue was diced into approximately 1–2 mm^3 pieces using a scalpel. The tissue was then weighed and subsequently incubated with high glucose Dulbecco's modified Eagle medium (DMEM, Gibco) containing 750 U collagenase I (Gibco). For conventional isolation, the tissue was rotated at 10 rotations per minute (RPM) at 37 °C for ~3 hours until over 90 % of the original tissue was broken down. For rapid isolation, the tissue was shaken at 2000 RPM at 37 °C for 30 minutes (Multi Reax Shaker, Heidolph, Schwabach, Bavaria, Germany). After digestion, DMEM containing 20 % fetal bovine serum (FBS, Gibco) was added to inactivate the collagenase. Insoluble tissue and residual fat were removed and discarded. The remaining cell suspension was passed through a series of cell strainers with decreasing mesh sizes (100 μm, 70 μm and 40 μm (Fisher Scientific)), centrifuged and washed with saline. Cells were then either plated for colony forming unit-fibroblast (CFU-F) analysis, prepared for cell surface marker analysis by magnetic activated cell sorting (MACS) or flow cytometry, or immediately seeded on AC-ECM scaffolds.

Flow Cytometry and Magnetic Activated Cell Sorting

For staining of cells with fluorochrome-conjugated antibodies against extracellular markers, cells were harvested, washed in phosphate-buffered saline (PBS) and stained with amine-binding markers for dead cells (Fixable Viability Dye; ThermoFisher) for 30 minutes at 4 °C. Cells were then washed in PBS and centrifuged at 300 g for 5 minutes prior to staining with fluorochrome-conjugated antibodies for CD45, CD34, CD90, CD105, CD44 and CD73 (all ThermoFisher) for 15 minutes at room temperature (RT). Following extracellular staining, cells were washed in fluorescence-activated cell sorting (FACS) buffer (PBS + 1 % FBS), centrifuged at 300 × g and re-suspended in FACS buffer for acquisition. Acquisition was performed on either a BD FACS Canto II (Becton, Dickinson & Company, Franklin Lakes, NJ, USA) or BD LSR Fortessa, and analysis was performed with FlowJo v.10 software (BD). For magnetic activated cell sorting (MACS), after washing in MACS buffer (PBS with 0.5 % bovine serum albumin (BSA), and 2 mM ethylenediaminetetraacetic acid (EDTA)), cells were incubated with CD44 microbeads before being passed through a MACS manual separation column as per the manufacturer's instructions (all Miltenyi Biotec, North Rhine-Westphalia, Germany).

Articular Cartilage ECM (AC-ECM) Scaffold Fabrication

Scaffolds were fabricated as previously described [26,28]. Briefly, pepsin solubilized porcine AC was cross-linked with glyoxal (5 mM), poured into 5 mm × 3 mm moulds and lyophilized to create a scaffold which was then subjected to dehydrothermal treatment (115 °C, under vacuum for 24 hours). The resulting scaffolds were predominantly collagenous in nature, with the majority of sulfated glycosaminoglycan (sGAG) and DNA removed during scaffold fabrication. The scaffolds contained AC-ECM at a concentration of 10 mg/mL as this concentration was previously found to be optimal for supporting chondrogenic differentiation of culture expanded FPSCs [26].

In Vitro Cell Seeding and Culture

1×10^6 rapidly or conventionally isolated FPSCs were seeded dropwise onto individual scaffolds suspended in 25 μL of expansion media (DMEM with 10 % FBS and 1 % penicillin-streptomycin). FPSCs were allowed to attach to the scaffolds for 1 hour in an incubator at 37 °C. After FPSC attachment, 2.5 mL of chemically defined media (CDM) was added per well. CDM consisted of high glucose DMEM supplemented with 1 % penicillin-streptomycin, 100 μg/mL sodium pyruvate (Sigma), 40 μg/mL L-Proline (Sigma), 50 μg/mL L-ascorbic acid-2-phosphate (Sigma), 1.5 mg/mL BSA (Sigma), 1X insulin transferrin selenium (ITS- Gibco), 100 nM dexamethasone (Sigma) and 10 ng/mL transforming growth factor beta-3 (TGF-β3, ThermoFisher). The FPSC seeded constructs were maintained in CDM for 28 days.

Colony Forming Unit-Fibroblast (CFU-F) Assay

Freshly isolated FPSCs were seeded in dishes at a density of 25 cells/cm^2. FPSCs were cultured in expansion media which consisted of high glucose DMEM supplemented with 1 % penicillin-streptomycin and 10 % FBS (Gibco). Cell growth was monitored to ensure distinct colonies did not merge. After 10 days of culture, the expansion media was removed and dishes washed twice in PBS. Cells were then fixed with 2 % paraformaldehyde (PFA) for 15 minutes at RT. PFA was subsequently removed and the dishes washed with PBS. Colonies were then stained with 1 % crystal violet solution (Sigma) for 2 minutes at RT. Dishes were then rinsed with tap water to remove unbound stain. Images were acquired and the colonies manually counted.

In Vitro Study Analysis

FPSC seeded constructs (Day 28) were analysed for DNA and sGAG content. sGAG quantification was performed using a 1, 9 dimethylmethylene blue (DMMB) assay according to the manufacturer's protocol (Blyscan sulfated sGAG assay kit, B1000, BioColor, Belfast, Northern Ireland). Quantification of dsDNA in the digested constructs was performed using a Quant-iT Pico Green dsDNA kit (ThermoFisher) according to the manufacturer's protocol. The combination of results from the DMMB and picogreen assays provides a ratio of sGAG normalized to dsDNA content. For histological analysis, samples were sec-

tioned at a thickness of 5 μm using a microtome. Sections were stained with 1 % alcian blue to examine sulfated glycosaminoglycan (sGAG) and picrosirius red to examine collagen deposition. To identify the specific collagen types present in the constructs, immunohistochemistry was performed for collagen types II and X as previously described [30].

Surgical Procedure

The n for the goats used in this study was based on the predicted variance in the model and was powered to detect 0.05 significance. The implantation groups were randomised across the operated animals. N = 9 animals were operated on for each group. Unfortunately, 3 animals from each cohort died prior to the 6-month end-point. These animal deaths were deemed not to be related to the surgical procedure following post-mortem by a veterinarian. Prior to admittance onto the study, all animals were monitored and evaluated prior to surgery and deemed healthy prior to surgery, no animals that reached the 6 month timepoint were excluded the study or subsequent analysis. As animals received both controls and treatment groups no randomisation of the animals was performed but the location (left or right stifle) of control and treatment groups was randomized for each surgery. Surgery was performed on skeletally mature female Saanen goats (age 4.8 years $\pm$ 0.27; mean $\pm$ SD). Goats were placed in dorsal recumbency and an arthrotomy of each stifle joint was then performed using the lateral para-patellar approach as described previously [28,31]. Bi-lateral surgery was performed on all animals. IFP biopsies were harvested from all animals and transported to the laboratory in saline (0.9 % NaCl) for rapid FPSC isolation to commence. FPSCs were rapidly isolated as described above, 1×10^6 FPSCs were seeded onto each AC-ECM scaffold (6 mm Ø $\times$ 2 mm high) and then returned to the operating room for implantation. 6 mm diameter chondral defects were created in the medial femoral condyles using a 6 mm biopsy punch to mark the defect diameter followed by full thickness cartilage removal using a ring curette. MFX was performed on all defects (including scaffold treated groups) using a Kirschner wire (1.6 mm Ø for a central hole and 0.7 mm Ø for all other holes (gSource Surgical Instruments, Emerson, NJ, USA)) to perforate the subchondral bone. AC-ECM scaffolds were maintained in position using a custom made, biodegradable, 3D printed fixation device fabricated using polycaprolactone (PCL, Perstorp CAPA 6500, Malmö, Sweden) [28]. The shaft of the fixation device was fabricated to be the same diameter as the central MFX hole (1.6 mm Ø) so that the device and scaffold could be push-fit into the defect. Tissue repair was evaluated at 6 months post-surgery. Repair tissue in defects treated with the rapidly isolated FPSCs seeded on an AC-ECM scaffold (termed the "scaffold + FPSCs" group) were compared to that in defects treated with the AC-ECM scaffold alone (termed the "+ AC-ECM scaffold" group) or microfracture only (termed the "MFX" group). The AC-ECM scaffold alone and MFX group (n = 6) were also used as a shared control with other goat studies undertaken at the same time [28], this was in order to reduce the overall numbers of animals required for these studies in accordance with animal welfare principals of the reduction, replacement and refinement (Article 4 of EU Directive 2010/63/EU). Blinded scoring of gross morphology and histology was performed. For this scoring, the samples were randomised using a randomization algorithm and the identification numbers of the animals removed from the samples.

Evaluation of Repair Tissue

6 month post-operatively, 1.5 cm^3 sections containing the defect site were harvested from the medial femoral condyle using an oscillating saw. Before fixation, gross morphological images were taken with a digital microscope system (Ash Inspex HD 1080p, Kildare, Ireland) for macroscopic evaluation. Macroscopic images were blinded, randomised and subsequently scored by four expert reviewers using a previously described macroscopic scoring system [28,31,32]. Samples were then fixed using 4 % formalin solution for 48 hours and subsequently decalcified in Decal-lite (Sigma). Samples were sectioned at 10 μm and stained with safranin O and picrosirius red. Immunohistochemistry was performed for type II collagen (Santa Cruz-sc52658 1:400, Dallas, TX, USA) and lubricin (Merck Millipore MABT400 1:500) as previously described [26]. Histological scoring was performed using a modified International Cartilage Regeneration and Joint Preservation Society (ICRS) II scoring system [33]. In addition, semi-quantification of type II collagen immunohistochemistry, safranin O, and picrosirius red histological staining was performed as previously described [28,34]. Briefly, safranin O staining was used in combination with Photoshop CS6 (Adobe, Mountain View, CA, USA) to quantify the area of positively stained cartilage within a region of interest (ROI) in the AC. To quantify the extent of positive type II collagen staining in the defect site defect, a 2 $\times$ 6 mm region of interest central to the defect was selected and DAB (3,3′-diaminobenzidine) positive staining was quantified using the plugin IHC profiler for Image J [35]. Picrosirius red stained samples were imaged under polarized light microscopy to investigate collagen fibre orientation. The Directionality plugin [36] from Image J was used to quantify the mean orientation and angular dispersion of the collagen fibres observed in the superficial and deep zones of the regenerated AC.

Statistical Analysis

Results are presented as mean $\pm$ standard deviation unless noted otherwise in figure legends. Statistical analysis was performed using Graph Pad Prism 10 (GraphPad Software, San Diego, CA, USA). Statistical differences

were analysed by one-way analysis of variance (ANOVA) with Tukey's test for multiple comparisons to compare experimental conditions or in the case of comparing two experiment groups a paired or unpaired *t*-test was used when appropriate. Statistically significant changes are marked as $p \leq 0.05$; $p \leq 0.01$; $p \leq 0.001$.

Results

A Method to rapidly Isolate Colony Forming Stromal Cells from the Infrapatellar Fat Pad

A methodology was developed to isolate stromal cells from IFP obtained during total knee replacement or anterior cruciate ligament reconstruction surgery. The method combined both enzymatic and mechanical methods to rapidly isolate clinically relevant cell numbers. The protocol for obtaining a cell suspension ready for use took less than 60 minutes for the rapid method, compared to 3–3.5 hours for the conventional isolation method (Fig. 1**A**). Cell yield per gram of tissue revealed that the conventional method resulted in a mean yield of $1.8 \times 10^6 \pm 0.64 \times 10^6$ cells compared to $0.95 \times 10^6 \pm 0.24 \times 10^6$ cells per gram of IFP for the rapid method (Fig. 1**B**), although no statistical difference was observed ($p = 0.2403$). While use of the rapid method resulted in less total cell yield, further characterisation of these cells demonstrated that the rapidly isolated cells contained a higher proportion of cells with stem-like characteristics. MACS analysis of both cell populations revealed that a significantly greater proportion of CD44 positive cells was obtained using the rapid method (42 % ± 19 %) versus the conventional method (28 % ± 21 %) ($p = 0.0239$, Fig. 1**C**). Analysis of colonies formed during a CFU-F assay demonstrated that the rapid population contained a significantly higher proportion of colony forming cells (413 ± 79 colonies) versus the conventional control (240 ± 29 colonies) ($p = 0.0408$, Fig. 1**D,E**).

Surface Marker Expression of conventionally and rapidly Isolated Fat Pad Stromal Cells

Having developed a method to rapidly isolate stromal cells from the IFP, we next sought to further characterise and define the different cellular populations obtained from the IFP via conventional and rapid methods. In order to accurately assess a panel of surface markers, flow cytometry analysis was performed within 3 hours of tissue processing and cell isolation. FPSCs were defined as $CD45^-/CD34^-$ to distinguish them from haematopoietic and endothelial cells respectively [37,38], and typically represented >90 % of the total viable cell population (Fig. 2**A**). Importantly, cell viability was comparable for both isolation methods, with an average viability of 79.1 % ± 5.53 % and 82.9 % ± 4.94 % for conventional and rapid isolation respectively (Fig. 2**B**).

For further analysis, a panel of well-established MSC markers, CD90, CD105, CD73 and CD44 [24,39,40], was used to characterise these cells and revealed distinct differences in surface marker distributions depending on the isolation procedure. Both rapidly and conventionally isolated FPSCs were found to have a low comparable expression and percentage of cells positive for CD90 and CD105. However, differences in the percentage of cells positive for CD44 and CD73, and their level of expression, were observed. Conventionally isolated cells consisted of a larger population of $CD73^+$ cells (26.3 % ± 8.513 %) compared to that of rapidly isolated cells (10.9 % ± 4.73 %, $p = 0.0511$). Interestingly, while expression of this marker is used to define MSCs, it is associated with and highly expressed on stromal cells with a more adipogenic phenotype [41]. In contrast, rapidly isolated FPSCs contained a higher percentage of $CD44^+$ cells (18.8 % ± 2.196 %) compared to conventionally isolated cells (6.458 % ± 2.269 %, $p = 0.0079$), CD44 is a surface marker associated with chondroprogenitor cells [22,23,42]. This was observed for FPSCs isolated from 4 independent donors (Fig. 2**C,D**). Taken together, this data demonstrates that cell populations differ depending on the isolation procedure, with the rapidly isolated population containing a higher fraction of $CD44^+$ cells.

Rapidly Isolated Human FPSCs Possess a Greater Chondrogenic Capacity than conventionally Isolated FPSCs

Having demonstrated that the rapid cell isolation method resulted in a significantly greater proportion of CD44 positive cells, we next sought to assess the *in vitro* chondrogenic capacity of both cell populations. To this end, cells from three donors (A, B and C) were seeded onto AC-ECM derived scaffolds [26] immediately after the cell isolation procedure (i.e., no cell expansion on plastic was undertaken) and then maintained in chondrogenic culture conditions for 28 days. Rapidly isolated cells from Donors A and B both demonstrated robust chondrogenic potential, with abundant sGAG (alcian blue) and collagen (picrosirius red) deposition within the engineered tissues. Significantly greater levels of sGAG were measured in tissues formed from rapidly isolated cells from both donors when compared to (donor matched) conventionally isolated FPSCs (Donor A—$p = 0.0083$, Donor B—$p < 0.0001$). Moreover, the cartilage formed by the rapidly isolated FPSCs resembled hyaline cartilage, being rich in type II collagen with little to no type X collagen deposition observed (Fig. 3**A,E**). While donor C was observed to possess attenuated differentiation capacity in comparison to donors A and B (Fig. 3**I–L**), a 2.5 fold increase in the GAG: DNA ratio was still observed in the rapid FPSC group when compared to the conventionally isolated FPSCs ($p = 0.0612$, Fig. 3**L**). Increases in sGAG, DNA and GAG: DNA ratio were obsrerved across all three donors individually (Fig. 3**B–D, F–H, J–L**). When data from all three donors was pooled, biochemical quantification revealed that the tissues engineered using the rapidly isolated FPSCs contained signifi-

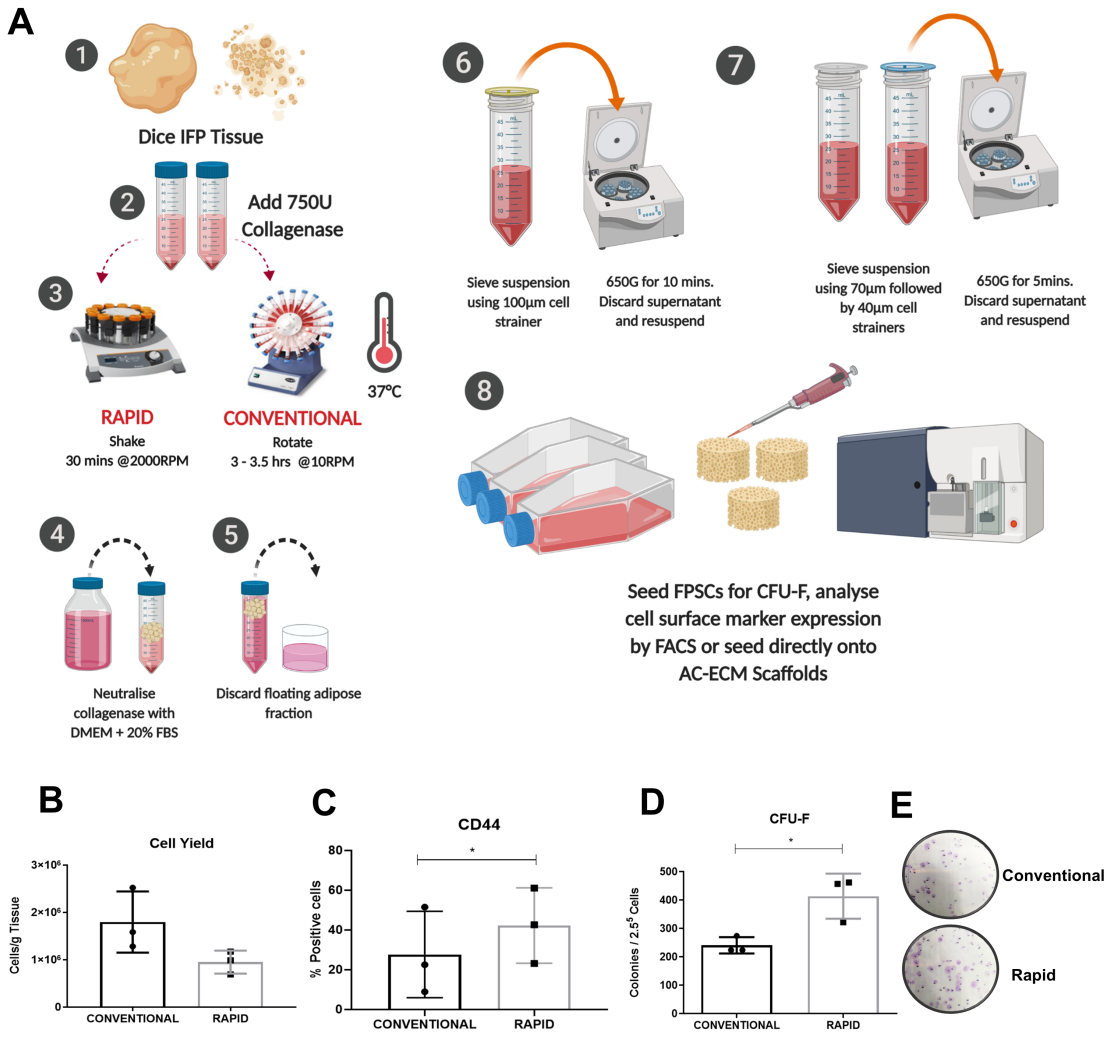

Fig. 1. A novel method to rapidly isolate infrapatellar fat pad stromal cells. (**A**) Schematic diagram illustrating the clinical workflow for the rapid and conventional isolation procedures from tissue biopsy to single-cell suspension. (**B**) Viable cell yield of FPSCs per gram of initial IFP tissue mass. (**C**) MACS was performed on the total conventional or rapid cell population's immediately after the isolation procedure. MACS separated the FPSCs into CD44 positive and negative fraction and cell counts were performed to quantify cell numbers. (**D**) Quantification of numbers of colonies observed after CFU-F assay. (**E**) CFU-F assay—Tissue culture plates were stained with crystal violet to reveal presence of colonies. All error bars denote standard deviation, $*p < 0.05$, n = 3 independent human donors. Schmatic diargram created with https://www.biorender.com. IFP, infrapatellar fat pad; RPM, rotations per minute; DMEM, Dulbecco's modified Eagle medium; FBS, fetal bovine serum; FPSC, fat pad stromal cell; CFU-F, colony forming unit-fibroblast; AC-ECM, articular cartilage extracellular matrix; MACS, magnetic activated cell sorting.

cantly greater levels of total sGAG ($p = 0.0002$) and sGAG: DNA ($p = 0.0028$) levels when compared to tissues generated using conventionally isolated FPSCs (Fig. 3**M–O**).

The Incorporation of rapidly Isolated FPSCs Seeded onto Extracellular Matrix Derived Scaffolds Does not Further Enhance Their Regenerative Potential in a clinically Relevant Large Animal Model

Having demonstrated that rapidly isolated human FPSCs can readily undergo robust chondrogenic differentiation *in vitro*, generating higher levels of hyaline-like cartilage matrix compared to conventionally isolated cells. We

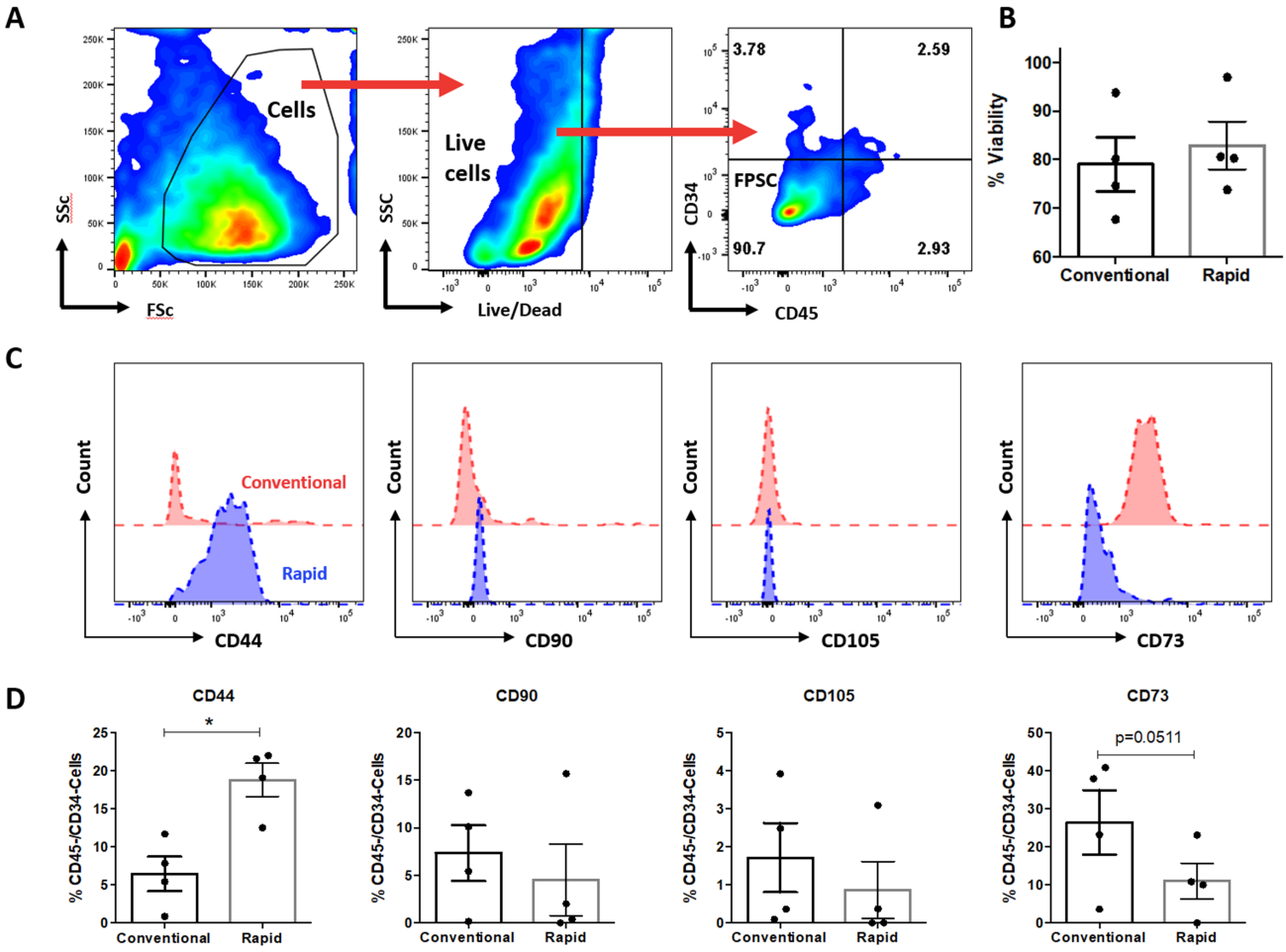

Fig. 2. Rapidly isolated FPSCs express higher levels of CD44 compared to conventionally isolated FPSCs. Human fat pad stromal cells (FPSCs) were isolated as described by either rapid or conventional isolation protocols. Isolated cells were stained with fluorochrome-conjugated antibodies against CD45, CD34, CD44, CD90, CD105 and CD73 and analysed by flow cytometry. (**A**) Cells were first selected by FSC and SSC, viable cells were then selected on the basis of viability dye exclusion. $CD45^{-}/CD34^{-}$ cells were selected for as the FPSC population. (**B**) Percentage viability of conventionally or rapidly isolate cells based on viability exclusion dye (n = 4 donors). (**C**) Representative histograms for each cell surface marker expression for conventional (red) and rapid (blue) isolation methods. (**D**) Pooled data depicting the mean (± SEM) percentage cells expressing CD44, CD90, CD105 and CD73 for 4 human independent donors. *$p < 0.05$.

next sought to assess the regenerative potential of rapidly isolated caprine FPSCs, when seeded onto AC-ECM scaffolds, in a clinically relevant large animal model of cartilage defect repair. A Schematic diagram of the design and timeline of *in vivo* experiment is provided in Fig. 4**A** (Ref. [28]). Six months post-implantation, animals were euthanized, and chondral defect repair was evaluated (Fig. 4**B–D**). As a current surgical standard of care, microfracture (MFX) treated animals acted as the positive control for this study (Fig. 4**B**). In addition, data from control animals treated with the AC-ECM scaffold alone are also provided (Fig. 4**C**). The quality of the repair tissue was found to be variable across both the MFX, AC-ECM scaffold alone and scaffold + FPSCs groups. Some MFX only animals were found to have high levels of defect fill, and this was reflected in gross morphology scoring and visualised by safranin-O histological staining (Fig. 4**B** & Fig. 5**A** (Ref. [28])). Over 40 % of the animals that received MFX only

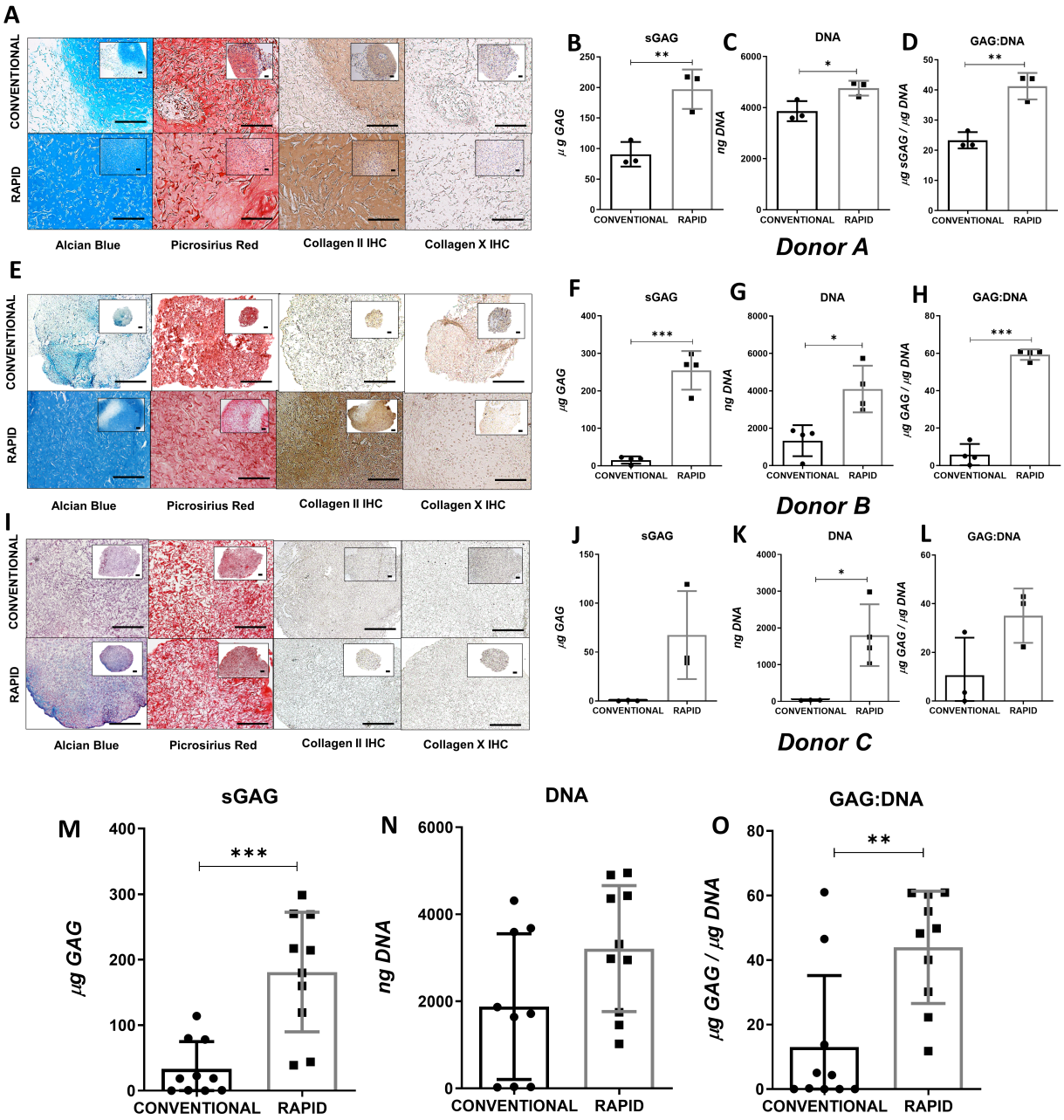

Fig. 3. Rapidly isolated human FPSCs possess greater chondrogenic capacity than conventionally isolated FPSCs. 1×10^6 rapidly or conventionally isolated FPSCs were cultured in AC-ECM biomaterial scaffolds for 28 days. sGAG deposition (alcian blue), collagen deposition (picrosirius red) and type II/X collagen deposition was evaluated by histological and immunohistochemical staining of day 28 FPSC seeded scaffold constructs (**A, E and I**). Biochemical quantification of DNA, sGAG and sGAG: DNA ratio was performed on day 28 constructs (**Donors A, B & C individually—panels B–D, F–H, J–L and in combination M–O**). (**G**) All error bars denote standard deviation, *$p < 0.05$, **$p < 0.01$, ***$p < 0.001$. N = 3 independent human donors, 3/4 constructs per group. Scale bars =200 μm. sGAG, sulfated glycosaminoglycan.

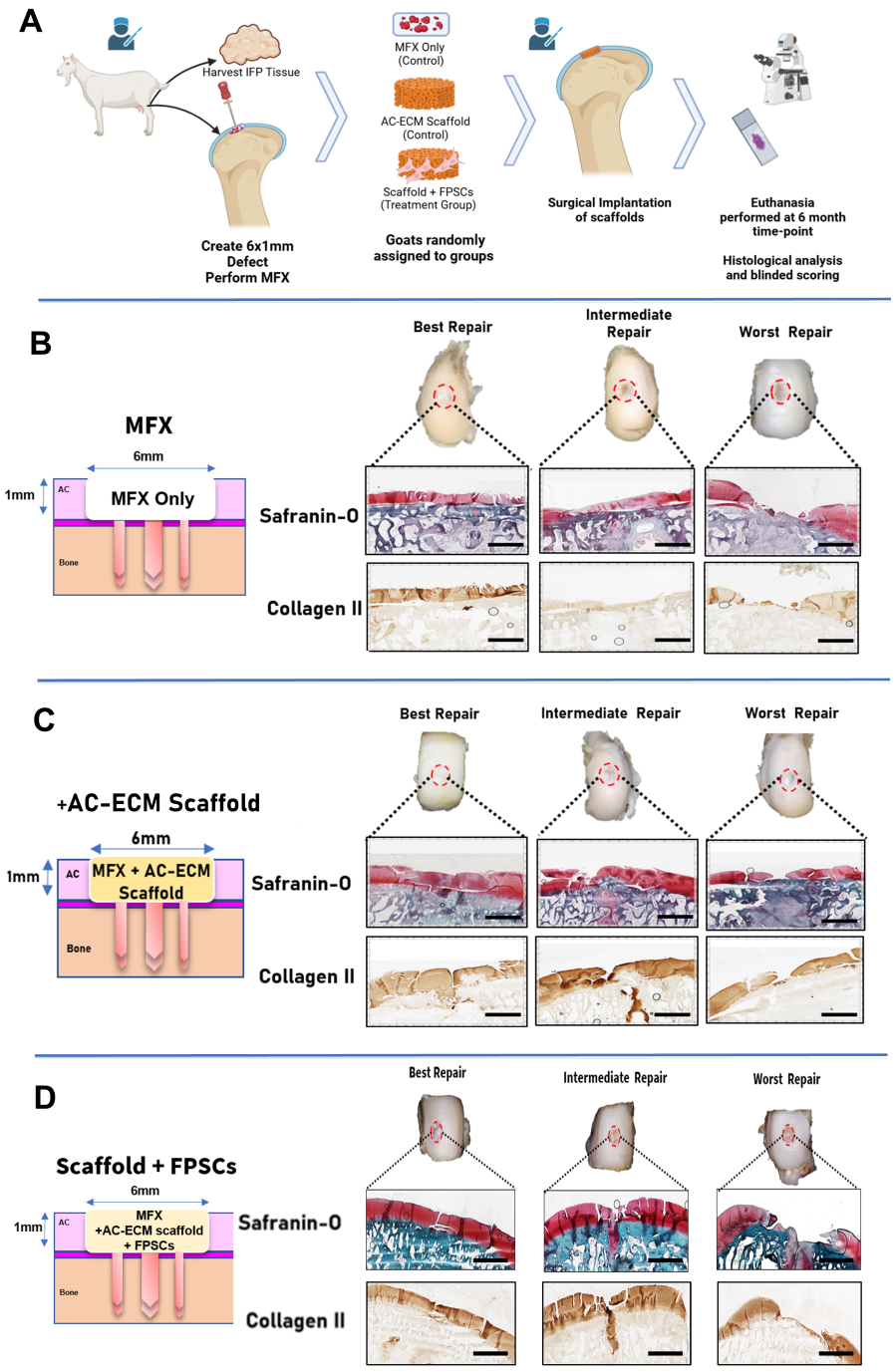

Fig. 4. Histoligical Evaluation of efficacy of rapidly isolated caprine FPSCs seeded on an AC-ECM scaffold in a preclinical model. 6 months after implantation, the defect sites were excised, imaged and processed for histology. (**A**) Schematic diagram of the design and timeline of *in vivo* experiment. (**B**) MFX only treated animals exhibited high variation in defect fill and repair quality. (**C**) MFX + AC-ECM scaffold treated animals showed enhanced repair quality compared to MFX only controls. (**D**) Scaffold + FPSCs treated animals demonstrated further improved and more consistent repair quality when compared to both MFX only and MFX + AC-ECM controls. Note: In order to reduce the overall numbers of animals required for these studies in accordance with animal welfare principals of the reduction, replacement and refinement (Article 4 of EU Directive 2010/63/EU) the data for the controls (MFX and + AC-ECM Scaffold groups) in the large animal study have been shared with our recently published study—Browe *et al*. [28] "Promoting endogenous articular cartilage regeneration using extracellular matrix scaffolds" Materials Today Bio 16 (2022): 100343. As such, images in panels **B** and **C** have been reused from that publication. Scale bar = 2 mm in safranin-O and collagen II. N = 6 animals. MFX, microfracture.

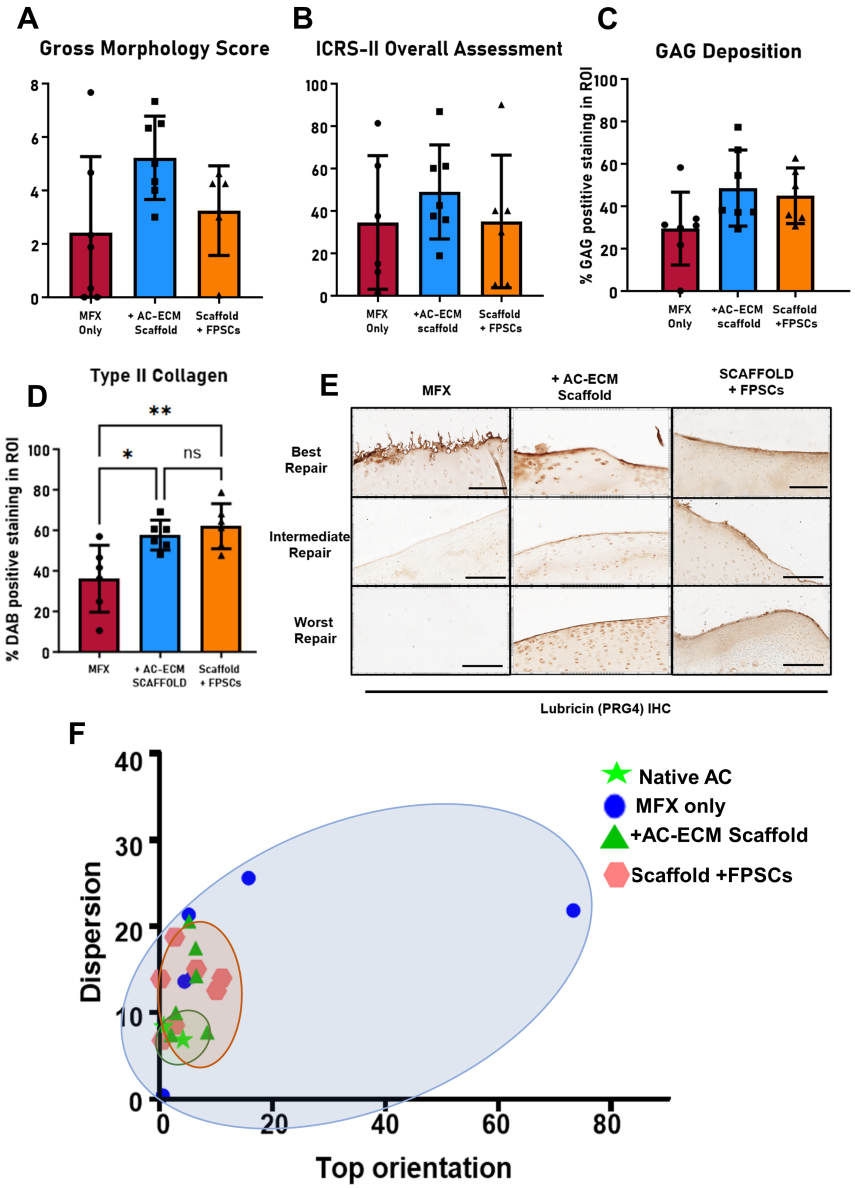

Fig. 5. Further Evaluation of efficacy of rapidly isolated caprine FPSCs seeded on an AC-ECM scaffold in a preclinical model. **(A)** Blinded macroscopic scoring was used to quantify visual repair of the defects ICRS-II histological scoring **(B)** was performed by 4 blinded experts. sGAG (**C**) and type II collagen (**D**) deposition within the defect region of interest was quantified using image analysis software. **(E)** Immunohistochemistry for lubricin. **(F)** The orientation and dispersion of the collagen fibre orientation of the superficial zone of the defect site relative to native controls was plotted. A lower dispersion value indicates higher consistency within the region of interest. Collagen fibres that run parallel to the articulating surface have an orientation of 0°, whereas fibres that are perpendicular to the surface have an orientation of 90° in native caprine cartilage tissue. Note: In order to reduce the overall numbers of animals required for these studies in accordance with animal welfare principals of the reduction, replacement and refinement (Article 4 of EU Directive 2010/63/EU) the data for the controls (MFX and + AC-ECM scaffold groups) in the large animal study have been shared with our recently published study—Browe *et al.* [28] "Promoting endogenous articular cartilage regeneration using extracellular matrix scaffolds" Materials Today Bio 16 (2022): 100343. As such, images in panels **E** have been reused from that publication. All error bars denote standard deviation. Scale bar = 200 μm for lubricin IHC. N = 6 animals. *$p < 0.05$, **$p < 0.01$. ROI, region of interest; DAB, 3,3′-diaminobenzidine; PGR4, proteoglycan 4; AC, articular cartilage; ICRS, International Cartilage Regeneration and Joint Preservation Society.

scored less than 1 point out of 8 when the gross morphology of the defect was scored; this low score translated into poor levels of actual defect fill with de novo tissue (Fig. 4**B** & Fig. 5**A**). More consistent levels of defect repair were observed in animals treated with AC-ECM scaffold alone and scaffold + FPSCs. Increasing scores in both gross morphology MFX: 2.4 points (± 2.64), AC-ECM scaffold only: 5.2 points (± 1.56), scaffold + FPSCs: 3.2 points (± 1.42) (see **Supplementary Table 1**) and sGAG positive staining in the defect site MFX only: 29 % (± 15.95), AC-ECM scaffold only: 48 % (± 17.89), scaffold + FPSCs: 45 % (± 13.11) were observed for the scaffold groups versus MFX only controls (Fig. 5**A,C**). Histological evaluation of the repair tissue using the ICRS-II scoring system did not reveal any significant differences between the treatment groups (Fig. 5**B** and **Supplementary Table 2**). Significantly higher levels of type II collagen deposition were observed in scaffold treated defects after 6 months *in vivo* (MFX—36 % of ROI stained positive; AC-ECM—58 % of ROI stained positive ($p = 0.0219$); scaffold + FPSCs—62 % of ROI stained positive $p = 0.0059$) when compared to MFX only controls. While an increase in type II collagen deposition was observed with the addition of FPSCs, this was not significant ($p = 0.8048$, Fig. 5**D**).

In this case the addition of the cells had no significant, beneficial effect on the repair parameters examined, with the AC-ECM scaffold only group scoring higher than the scaffold + FPSCs group in the three of four metrics examined. Recapitulation of the superficial zone of AC is crucial for the long-term success of any cartilage repair procedure. To further analyse the recapitulation of the superficial zone of the repair tissue, we next performed immunohistochemistry for lubricin (also known as proteoglycan 4 (PRG4)), a key protein expressed in the superficial zone of native, healthy AC [43,44]. Examining a central region in the defect site, we observed strong, specific lubricin staining in defects treated with scaffold only and scaffold + FPSCs. In contrast, the superficial zone of the majority of animals treated with MFX expressed lubricin non-specifically or weakly (Fig. 5**E**).

Following picrosirius red staining of histological samples, the samples underwent polarised light microscopy (PLM) to visually determine the collagen fibre orientation in the superficial zone (Fig. 5**F**). The degree of orientation and the dispersion of the collagen fibre orientation was quantified using the ImageJ plugin *Directionality* [28,29,45]. Native caprine cartilage has a parallel fibre orientation in the superficial zone, with the majority of fibres having an orientation approaching 0° and a low level of dispersion [45]. Representative native caprine values are contained in the green ellipse (Fig. 5**F**). Here we demonstrate that MFX only treated animals possess high levels of variation in both fibre dispersion and fibre orientation, as illustrated by the blue ellipse (Fig. 5**F**). However, when animals were treated with both the AC-ECM scaffold only or the scaffold + FPSCs, both the mean angle of collagen fibre orientation and fibre dispersion were seen to better match native values, as illustrated by the green and pink ellipses respectively (Fig. 5**F**). When quantified, the MFX only group had a mean fibre orientation angle of 17° (± 25°) with a mean dispersion value of 16.3 (± 8.3). In contrast, the scaffold + FPSCs group had a mean fibre orientation angle of 5° (± 4°) with a mean dispersion value of 12.9 (± 3.7).

Discussion

The overall goal of this study was to develop and preclinically assess a novel single-stage, intraoperative cartilage repair therapy. To this end, we developed a method to rapidly isolate clinically relevant numbers of FPSCs from human IFP tissue in under one hour. We next characterised the phenotype of the isolated cells and compared the chondrogenic potential of both rapidly and conventionally isolated FPSCs *in vitro*. We observed that the rapidly isolated cells contained both a higher proportion of colony-forming cells and had a greater chondrogenic capacity than conventionally isolated donor matched controls. Having developed this methodology, we then tested the ability of the rapidly isolated FPSCs, when combined with an AC-ECM-derived scaffold, to promote cartilage repair in a clinically relevant caprine model. In our preclinical model, the scaffold + Rapidly FPSC treatment improved tissue repair outcomes when compared with MFX only, recapitulating certain aspects of the zonal structure of AC. However we could not conclude that the delivery of such cells improved outcomes compared to implantation of the AC-ECM scaffold alone.

In vitro, rapidly isolated FPSCs from donors A and B were found to be highly chondrogenic upon seeding onto AC-ECM scaffolds. Not only were the rapidly isolated cells more chondrogenic than conventionally isolated cells from the same donor, but our previous data demonstrates that they were also more chondrogenic (>200 μg versus ~120 μg mean sGAG production per construct) than culture expanded FPSCs from healthy donors seeded on the same scaffolds as used in a previous study [26]. It may be that the rapid isolation procedure is preferentially selecting for the perivascular stem cells that are known to exist with the IFP [20], with other stromal cell populations also being isolated during the longer, conventional isolation protocol. Reduced time of exposure to collagenase may also be a factor for the improved performance of the rapidly isolated FPSCs, as prolonged time in collagenase has been shown to reduce cell viability and cell surface marker expression in cells derived from adipose, umbilical cord and other tissues [46–51]. Further time course studies are required to confirm this hypothesis in our system. Ideally, FPSCs would be isolated without the use of enzymatic products. Previous research has successfully isolated cells from adipose tissue using mechanical means only [52], however we ob-

served that we were unable to isolate sufficient, clinically relevant numbers using mechanical methods only in preliminary studies (data not shown). Obtaining sufficient cell numbers is a key parameter in order to translate a one-step cell therapeutic to the clinic. Here, we demonstrate that we can rapidly isolate approximately 1×10^6 cells per gram of human IFP tissue in under one hour. While less cells were obtained compared to using conventional methods, we were able to isolate greater cell numbers than published studies also attempting to use freshly isolated cells from IFP tissue [15]. Approximately 1×10^6 cells per gram of human IFP tissue can be obtained using our rapid method, of which approximately 20 % of these cells are $CD44^+$. Human AC contains chondrocytes at a density of 9600 cells per mm^3 and in order to regenerate damaged AC it could be assumed that at least an equivalent cell density would be required [15,53]. The cell seeding density used in this study was relatively low (1×10^6 cells) to ensure that equal cell numbers could always be implanted into each animal due to potential animal to animal IFP mass and cell yield variation. Similar caprine research has examined cell-seeding densities approximately 5 times higher (5×10^6 cells in a scaffold with a volume of 59 mm^3) than those used in this study (1×10^6 cells in a scaffold with a volume of 57 mm^3) when cell to scaffold volumes ratios are compared [54]. When the procedure is applied to humans (with an average IFP mass of approximately 15 g), a higher cell seeding density could be utilized, as a larger IFP biopsy can be obtained from the patient [15]. However, a relatively low cell seeding density may make the translation of the method to the clinic more attractive as only a small biopsy of IFP would need to be harvested to obtain sufficient cell numbers. Using the cell seeding density tested here, scaled to a clinically relevant 2 cm^3 chondral defect, would require an IFP biopsy of approximately 3.5 g. Further studies are required to identify the optimal cell seeding density for such single stage approaches.

Despite technology advancements, MFX remains the first line, surgical standard of care for many orthopaedic surgeons, as it has the benefits of being cost effective with a short surgical time [2,55]. However, the repair tissue observed is predominantly fibro-cartilaginous and this can result in deterioration of the repair tissue between 18–24 months post-surgery [56]. In turn, this results in high rates of revision surgery after MFX, and in some cohorts up to a quarter of patients required revision surgery just 18 months after the initial procedure [57]. In this study, we observed high animal-to-animal variation in the levels of repair following MFX, mimicking what is observed in humans. Although significant differences between the groups examined were not observed, defects treated with an AC-ECM scaffold were found to have higher levels of sGAG deposition and greater defect fill in the defect site when compared to MFX only controls. While greater levels of type II collagen deposition were observed with the addition of the FPSCs to the scaffold, this effect was not found to be statistically significant. In addition to lubricin expression, we also examined collagen fibre alignment in the superficial zone of the repair tissue to determine the addition of the FPSCs promoted recapitulation the defined collagen fibre orientation of native articular cartilage. This hierarchical structure of AC is responsible for the load bearing, wear resistance and shock absorption properties of the tissue [58]. We were able to demonstrate that the average angle of fibre orientation, as well as the level of fibre dispersion, was more akin to the native tissue in scaffold treated defects but the addition of the FPSCs did not further improve this metric. Previous research has demonstrated that collagen fibre alignment can continue to improve between 6 and 12 months post scaffold implantation [45], therefore it could be postulated that further improvements in collagen fibre orientation may be observed when longer time-points are examined. We observed positive lubricin staining in the superficial zone of defects treated with AC-ECM scaffolds both in the scaffold alone and the scaffold + FPSCs treated groups. This result was not observed in the MFX group. Lubricin (also known as superficial zone protein (SZP) or proteoglycan 4 (PGR4)) is a critical protein in healthy articular cartilage as it is responsible for coating the cartilage surface and providing boundary lubrication [43].

The addition of rapidly isolated caprine FPSCs did not result in significant improvements in repair outcomes *in vivo* compared to scaffold treatment alone, as assessed by macroscopic and histological scoring. One potential reason for this may be the age of the goat FPSCs used for the study. During the course of the *in vitro* study, we observed that for the diseased human samples to be able to undergo chondrogenic differentiation, the donor must be less than 60 years old. We were able to isolate viable FPSCs from several older human donors but they did not differentiate or proliferate in culture (data not shown). It has been well established that differentiation capacity of stem/stromal cells decreases with age [59–61]. This correlates with our *in vitro* differentiation findings where we observed the youngest donor tested (Donor B) possessed the greatest chondrogenic differentiation capacity as demonstrated by the highest sGAG levels; this was in contrast to the oldest donor (Donor C) that had the poorest capacity. Therefore, the approach may not be a viable treatment option for an older patient population if autologous cells are used. Therefore, we believe that this strategy is ideally suited to the treatment of younger patients who have suffered damage to the articular surface and are susceptible to the onset of post-traumatic OA. The goats used in the preclinical study were formerly dairy goats, which had come to the end of their milk production capabilities and thus alluding to their advanced age. Future studies are therefore required to assess the benefits of delivering rapidly isolated FPSCs derived from younger animals which may better represent the potential clinical patient cohort. Alternatively, studies could also look to assess

the regenerative capacity of rapidly isolated human FPSCs in the same goat model of cartilage repair.

Conclusions

In summary, there is an unmet need for biological cartilage repair strategies that are cost effective, have a short surgical time and are efficacious. We have developed a new cartilage repair therapy using rapidly isolated FPSCs, however further work is required to determine how factors such as patient age and cell-seeding density influence the efficacy of such an approach. With improvements in efficacy, such rapid isolation technology could be readily translated to the clinic, with the potential to be used with any commercially available cartilage repair scaffold products.

List of Abbreviations

AC, articular cartilage; AC-ECM, articular cartilage extracellular matrix; ACL, anterior cruciate ligament; ACI, autologous chondrocyte implantation; BMSC, bone marrow-derived stromal cell; CFU-F, colony forming unit-fibroblast; CDM, chemically defined media; DAB, 3,3′-diaminobenzidine; DMMB, dimethylmethylene blue; DMEM, Dulbecco's modified Eagle medium; ECM, extracellular matrix; FBS, fetal bovine serum; FPSC, fat pad stromal cell; IFP, infrapatellar fat pad; ICRS, International Cartilage Regeneration and Joint Preservation Society; MACI, matrix-assisted autologous chondrocyte implantation; MACS, magnetic activated cell sorting; MFX, microfracture; PBS, phosphate-buffered saline; PCL, polycaprolactone; PFA, paraformaldehyde; PGR4, proteoglycan 4; ROI, region of interest; RPM, rotations per minute; sGAG, sulfated glycosaminoglycan; SZP, superficial zone protein; TGF-β3, transforming growth factor beta-3; BSA, bovine serum albumin; RT, room temperature.

Availability of Data and Materials

The data used to support the findings of this study are available from the corresponding author upon request.

Author Contributions

DCB, ORM, PJDP, RB, FEF, JMN, PP, GG and PAJB performed the studies, analysed the data, reviewed and edited the manuscript. DCB and DJK designed the studies and wrote the initial draft of the manuscript. AD, CJM, PAJB, CTB and DJK analysed the data, reviewed and edited the manuscript, provided scientific direction and funding. All authors read and approved the final manuscript. All authors agreed to be accountable for all aspects of the work in ensuring that questions related to the accuracy or integrity of any part of the work were appropriately investigated and resolved.

Ethics Approval and Consent to Participate

Human tissue donations were approved by the Research Ethics Committee of the Sports Surgery Clinic, Santry, Dublin, Ireland and informed consent from patients was obtained prior to surgery. All animal experiments were approved by the University College Dublin Animal Research Ethics Committee (approval number: AREC 12-74) and the Irish Health Products Regulatory Authority (approval number: AE18982/P032).

Acknowledgments

The authors wish to thank the surgical and anaesthesia staff and students from the School of Veterinary Medicine, University College Dublin for their assistance with the animal studies.

Funding

Funding for the project was received from Enterprise Ireland (CF/2014/4325), Science Foundation Ireland through the Investigators Programme (12/IA/1554) and by the European Research Council (ANCHOR–779909, StemRepair–258463 and JointPrinting–647004). This research was co-funded by the European Regional Development Fund (ERDF) under Ireland's European Structural and Investment Funds Programmes 2014–2020.

Conflict of Interest

DCB, CTB and DJK are all co-founders and equity holders in Altach Biomedical Ltd. and are listed as inventors on patents related to the ECM scaffold technology described in this manuscript. Altach Biomedical Ltd. was founded after the completion of this study, it did not sponsor this study nor was the company involved in its design, implementation or analysis.

Research undertaken in Daniel Kelly's laboratory at Trinity College Dublin is part-funded by Johnson & Johnson 3D Printing Innovation & Customer Solutions, Johnson & Johnson Services Inc. This company did not sponsor this study and was not in any way involved in its design, implementation or analysis.

Supplementary Material

Supplementary material associated with this article can be found, in the online version, at https://doi.org/10.22203/eCM.v050a04.

References

[1] Brittberg M. Clinical articular cartilage repair—an up to date review. Annals of Joint. 2018; 3: 94. https://doi.org/10.21037/aoj.2018.11.09.

[2] Makris EA, Gomoll AH, Malizos KN, Hu JC, Athanasiou KA. Repair and tissue engineering techniques for articular cartilage. Nature Reviews. Rheumatology. 2015; 11: 21–34. https://doi.org/10.1038/nrrheum.2014.157.

[3] Gudas R, Kalesinskas RJ, Kimtys V, Stankevicius E, Toliusis V,

Bernotavicius G, *et al*. A prospective randomized clinical study of mosaic osteochondral autologous transplantation versus microfracture for the treatment of osteochondral defects in the knee joint in young athletes. Arthroscopy: the Journal of Arthroscopic & Related Surgery: Official Publication of the Arthroscopy Association of North America and the International Arthroscopy Association. 2005; 21: 1066–1075. https://doi.org/10.1016/j.arthro.2005.06.018.

[4] Knutsen G, Engebretsen L, Ludvigsen TC, Drogset JO, Grøntvedt T, Solheim E, *et al*. Autologous chondrocyte implantation compared with microfracture in the knee. A randomized trial. The Journal of Bone and Joint Surgery. American Volume. 2004; 86: 455–464. https://doi.org/10.2106/00004623-200403000-00001.

[5] Steadman JR, Briggs KK, Rodrigo JJ, Kocher MS, Gill TJ, Rodkey WG. Outcomes of microfracture for traumatic chondral defects of the knee: average 11-year follow-up. Arthroscopy: the Journal of Arthroscopic & Related surgery: Official Publication of the Arthroscopy Association of North America and the International Arthroscopy Association. 2003; 19: 477–484. https://doi.org/10.1053/jars.2003.50112.

[6] Pestka JM, Bode G, Salzmann G, Südkamp NP, Niemeyer P. Clinical outcome of autologous chondrocyte implantation for failed microfracture treatment of full-thickness cartilage defects of the knee joint. The American Journal of Sports Medicine. 2012; 40: 325–331. https://doi.org/10.1177/0363546511425651.

[7] Minas T, Gomoll AH, Rosenberger R, Royce RO, Bryant T. Increased failure rate of autologous chondrocyte implantation after previous treatment with marrow stimulation techniques. The American Journal of Sports Medicine. 2009; 37: 902–908. https://doi.org/10.1177/0363546508330137.

[8] Driscoll D, Farnia S, Kefalas P, Maziarz RT. Concise Review: The High Cost of High Tech Medicine: Planning Ahead for Market Access. Stem Cells Translational Medicine. 2017; 6: 1723–1729. https://doi.org/10.1002/sctm.16-0487.

[9] Słynarski K, de Jong WC, Snow M, Hendriks JAA, Wilson CE, Verdonk P. Single-Stage Autologous Chondrocyte-Based Treatment for the Repair of Knee Cartilage Lesions: Two-Year Follow-up of a Prospective Single-Arm Multicenter Study. The American Journal of Sports Medicine. 2020; 48: 1327–1337. https://doi.org/10.1177/0363546520912444.

[10] Matricali GA, Dereymaeker GP, Luyten FP. Donor site morbidity after articular cartilage repair procedures: a review. Acta Orthopaedica Belgica. 2010; 76: 669–674.

[11] McCarthy HS, Richardson JB, Parker JCE, Roberts S. Evaluating Joint Morbidity after Chondral Harvest for Autologous Chondrocyte Implantation (ACI): A Study of ACI-Treated Ankles and Hips with a Knee Chondral Harvest. Cartilage. 2016; 7: 7–15. https://doi.org/10.1177/1947603515607963.

[12] Hendriks J, Guidoux J, Verdonk P, Widuchowski J, Snow M, Kruczyński J, *et al*. First clinical experience with INSTRUCT–a single surgery, autologous cell based technology for cartilage repair. In 2013 ICRS conference. Izmir. 2013.

[13] Slynarski K, Widuchowski W, Snow M, Weiss W, Kruczynski J, Hendriks J, *et al*. Primary chondrocytes and bone marrow cells on a 3D co-polymer scaffold: 2-year results of a prospective, multicenter, single-arm clinical trial in patients with cartilage defects of the knee. Revue de Chirurgie Orthopédique et Traumatologique. 2015; 101: e17–e18. https://doi.org/10.1016/j.rcot.2015.09.350.

[14] de Windt TS, Vonk LA, Slaper-Cortenbach ICM, Nizak R, van Rijen MHP, Saris DBF. Allogeneic MSCs and Recycled Autologous Chondrons Mixed in a One-Stage Cartilage Cell Transplantion: A First-in-Man Trial in 35 Patients. Stem Cells. 2017; 35: 1984–1993. https://doi.org/10.1002/stem.2657.

[15] Jurgens WJ, van Dijk A, Doulabi BZ, Niessen FB, Ritt MJ, van Milligen FJ, *et al*. Freshly isolated stromal cells from the infrapatellar fat pad are suitable for a one-step surgical procedure to regenerate cartilage tissue. Cytotherapy. 2009; 11: 1052–1064. https://doi.org/10.3109/14653240903219122.

[16] Vinardell T, Buckley CT, Thorpe SD, Kelly DJ. Composition-function relations of cartilaginous tissues engineered from chondrocytes and mesenchymal stem cells isolated from bone marrow and infrapatellar fat pad. Journal of Tissue Engineering and Regenerative Medicine. 2011; 5: 673–683. https://doi.org/10.1002/term.357.

[17] Vinardell T, Sheehy EJ, Buckley CT, Kelly DJ. A comparison of the functionality and *in vivo* phenotypic stability of cartilaginous tissues engineered from different stem cell sources. Tissue Engineering. Part A. 2012; 18: 1161–1170. https://doi.org/10.1089/ten.TEA.2011.0544.

[18] Almeida HV, Liu Y, Cunniffe GM, Mulhall KJ, Matsiko A, Buckley CT, *et al*. Controlled release of transforming growth factor-β3 from cartilage-extra-cellular-matrix-derived scaffolds to promote chondrogenesis of human-joint-tissue-derived stem cells. Acta Biomaterialia. 2014; 10: 4400–4409. https://doi.org/10.1016/j.actbio.2014.05.030.

[19] Liu Y, Buckley CT, Almeida HV, Mulhall KJ, Kelly DJ. Infrapatellar fat pad-derived stem cells maintain their chondrogenic capacity in disease and can be used to engineer cartilaginous grafts of clinically relevant dimensions. Tissue Engineering. Part A. 2014; 20: 3050–3062. https://doi.org/10.1089/ten.TEA.2014.0035.

[20] Hindle P, Khan N, Biant L, Péault B. The Infrapatellar Fat Pad as a Source of Perivascular Stem Cells with Increased Chondrogenic Potential for Regenerative Medicine. Stem Cells Translational Medicine. 2017; 6: 77–87. https://doi.org/10.5966/sctm.2016-0040.

[21] Francis SL, Duchi S, Onofrillo C, Di Bella C, Choong PFM. Adipose-Derived Mesenchymal Stem Cells in the Use of Cartilage Tissue Engineering: The Need for a Rapid Isolation Procedure. Stem Cells International. 2018; 2018: 8947548. https://doi.org/10.1155/2018/8947548.

[22] Ahearne M, Liu Y, Kelly DJ. Combining freshly isolated chondroprogenitor cells from the infrapatellar fat pad with a growth factor delivery hydrogel as a putative single stage therapy for articular cartilage repair. Tissue Engineering. Part A. 2014; 20: 930–939. https://doi.org/10.1089/ten.TEA.2013.0267.

[23] Almeida HV, Cunniffe GM, Vinardell T, Buckley CT, O'Brien FJ, Kelly DJ. Coupling Freshly Isolated CD44(+) Infrapatellar Fat Pad-Derived Stromal Cells with a TGF-β3 Eluting Cartilage ECM-Derived Scaffold as a Single-Stage Strategy for Promoting Chondrogenesis. Advanced Healthcare Materials. 2015; 4: 1043–1053. https://doi.org/10.1002/adhm.201400687.

[24] Tangchitphisut P, Srikaew N, Numhom S, Tangprasittipap A, Woratanarat P, Wongsak S, *et al*. Infrapatellar Fat Pad: An Alternative Source of Adipose-Derived Mesenchymal Stem Cells. Arthritis. 2016; 2016: 4019873. https://doi.org/10.1155/2016/4019873.

[25] Duchi S, Francis SL, Onofrillo C, O'Connell CD, Choong P, Di Bella C. Towards Clinical Translation of *In Situ* Cartilage Engineering Strategies: Optimizing the Critical Facets of a Cell-Laden Hydrogel Therapy. Tissue Engineering and Regenerative Medicine. 2023; 20: 25–47. https://doi.org/10.1007/s13770-022-00487-9.

[26] Browe DC, Mahon OR, Díaz-Payno PJ, Cassidy N, Dudurych I, Dunne A, *et al*. Glyoxal cross-linking of solubilized extracellular matrix to produce highly porous, elastic, and chondro-permissive scaffolds for orthopedic tissue engineering. Journal of Biomedical Materials Research. Part A. 2019; 107: 2222–2234. https://doi.org/10.1002/jbm.a.36731.

[27] Mahon OR, Browe DC, Díaz-Payno PJ, Pitacco P, Cunningham KT, Mills KHG, *et al*. Extracellular matrix scaffolds derived from different musculoskeletal tissues drive distinct macrophage phenotypes and direct tissue-specific cellular differentiation. Journal of Immunology and Regenerative Medicine. 2021; 12: 100041. https://doi.org/10.1016/j.regen.2021.100041.

[28] Browe DC, Burdis R, Díaz-Payno PJ, Freeman FE, Nulty JM, Buckley CT, *et al*. Promoting endogenous articular cartilage regeneration using extracellular matrix scaffolds. Materials Today. Bio. 2022; 16:

100343. https://doi.org/10.1016/j.mtbio.2022.100343.
[29] Browe DC, Díaz-Payno PJ, Freeman FE, Schipani R, Burdis R, Ahern DP, *et al*. Bilayered extracellular matrix derived scaffolds with anisotropic pore architecture guide tissue organization during osteochondral defect repair. Acta Biomaterialia. 2022; 143: 266–281. https://doi.org/10.1016/j.actbio.2022.03.009.
[30] Buckley CT, Vinardell T, Thorpe SD, Haugh MG, Jones E, McGonagle D, *et al*. Functional properties of cartilaginous tissues engineered from infrapatellar fat pad-derived mesenchymal stem cells. Journal of Biomechanics. 2010; 43: 920–926. https://doi.org/10.1016/j.jbiomech.2009.11.005.
[31] Levingstone TJ, Ramesh A, Brady RT, Brama PAJ, Kearney C, Gleeson JP, *et al*. Cell-free multi-layered collagen-based scaffolds demonstrate layer specific regeneration of functional osteochondral tissue in caprine joints. Biomaterials. 2016; 87: 69–81. https://doi.org/10.1016/j.biomaterials.2016.02.006.
[32] Getgood AM, Kew SJ, Brooks R, Aberman H, Simon T, Lynn AK, *et al*. Evaluation of early-stage osteochondral defect repair using a biphasic scaffold based on a collagen–glycosaminoglycan biopolymer in a caprine model. The Knee. 2012; 19: 422–430. https://doi.org/10.1016/j.knee.2011.03.011.
[33] Mainil-Varlet P, Van Damme B, Nesic D, Knutsen G, Kandel R, Roberts S. A new histology scoring system for the assessment of the quality of human cartilage repair: ICRS II. The American Journal of Sports Medicine. 2010; 38: 880–890. https://doi.org/10.1177/0363546509359068.
[34] Díaz-Payno PJ, Browe DC, Cunniffe GM, Kelly DJ. The identification of articular cartilage and growth plate extracellular matrix-specific proteins supportive of either osteogenesis or stable chondrogenesis of stem cells. Biochemical and Biophysical Research Communications. 2020; 528: 285–291. https://doi.org/10.1016/j.bbrc.2020.05.074.
[35] Varghese F, Bukhari AB, Malhotra R, De A. IHC Profiler: an open source plugin for the quantitative evaluation and automated scoring of immunohistochemistry images of human tissue samples. PLoS One. 2014; 9: e96801. https://doi.org/10.1371/journal.pone.0096801.
[36] Reznikov N, Almany-Magal R, Shahar R, Weiner S. Three-dimensional imaging of collagen fibril organization in rat circumferential lamellar bone using a dual beam electron microscope reveals ordered and disordered sub-lamellar structures. Bone. 2013; 52: 676–683. https://doi.org/10.1016/j.bone.2012.10.034.
[37] Dominici M, Le Blanc K, Mueller I, Slaper-Cortenbach I, Marini F, Krause D, *et al*. Minimal criteria for defining multipotent mesenchymal stromal cells. The International Society for Cellular Therapy position statement. Cytotherapy. 2006; 8: 315–317. https://doi.org/10.1080/14653240600855905.
[38] Breitbach M, Kimura K, Luis TC, Fuegemann CJ, Woll PS, Hesse M, *et al*. *In Vivo* Labeling by CD73 Marks Multipotent Stromal Cells and Highlights Endothelial Heterogeneity in the Bone Marrow Niche. Cell Stem Cell. 2018; 22: 262–276. e7. https://doi.org/10.1016/j.stem.2018.01.008.
[39] Kouroupis D, Bowles AC, Willman MA, Perucca Orfei C, Colombini A, Best TM, *et al*. Infrapatellar fat pad-derived MSC response to inflammation and fibrosis induces an immunomodulatory phenotype involving CD10-mediated Substance P degradation. Scientific Reports. 2019; 9: 10864. https://doi.org/10.1038/s41598-019-47391-2.
[40] Schachtele S, Clouser C, Aho J. Markers and Methods to Verify Mesenchymal Stem Cell Identity, Potency, and Quality. R&D Systems. 2013; 10.
[41] Li Q, Qi LJ, Guo ZK, Li H, Zuo HB, Li NN. CD73+ adipose-derived mesenchymal stem cells possess higher potential to differentiate into cardiomyocytes *in vitro*. Journal of Molecular Histology. 2013; 44: 411–422. https://doi.org/10.1007/s10735-013-9492-9.
[42] O'Sullivan J, D'Arcy S, Barry FP, Murphy JM, Coleman CM. Mesenchymal chondroprogenitor cell origin and therapeutic potential. Stem Cell Research & Therapy. 2011; 2: 8. https://doi.org/10.1186/scrt49.
[43] Jay GD, Waller KA. The biology of lubricin: near frictionless joint motion. Matrix Biology: Journal of the International Society for Matrix Biology. 2014; 39: 17–24. https://doi.org/10.1016/j.matbio.2014.08.008.
[44] Schumacher BL, Block JA, Schmid TM, Aydelotte MB, Kuettner KE. A novel proteoglycan synthesized and secreted by chondrocytes of the superficial zone of articular cartilage. Archives of Biochemistry and Biophysics. 1994; 311: 144–152. https://doi.org/10.1006/abbi.1994.1219.
[45] Cunniffe GM, Díaz-Payno PJ, Sheehy EJ, Critchley SE, Almeida HV, Pitacco P, *et al*. Tissue-specific extracellular matrix scaffolds for the regeneration of spatially complex musculoskeletal tissues. Biomaterials. 2019; 188: 63–73. https://doi.org/10.1016/j.biomaterials.2018.09.044.
[46] Seaman SA, Tannan SC, Cao Y, Peirce SM, Lin KY. Differential Effects of Processing Time and Duration of Collagenase Digestion on Human and Murine Fat Grafts. Plastic and Reconstructive Surgery. 2015; 136: 189e–199e. https://doi.org/10.1097/PRS.0000000000001446.
[47] Feng X, Liu L, Yu BQ, Huang JM, Gu LD, Xu DF. Effect of optimized collagenase digestion on isolated and cultured nucleus pulposus cells in degenerated intervertebral discs. Medicine. 2018; 97: e12977. https://doi.org/10.1097/MD.0000000000012977.
[48] Yonenaga K, Nishizawa S, Fujihara Y, Asawa Y, Sanshiro K, Nagata S, *et al*. The optimal conditions of chondrocyte isolation and its seeding in the preparation for cartilage tissue engineering. Tissue Engineering. Part C, Methods. 2010; 16: 1461–1469. https://doi.org/10.1089/ten.TEC.2009.0597.
[49] Taghizadeh RR, Cetrulo KJ, Cetrulo CL. Collagenase Impacts the Quantity and Quality of Native Mesenchymal Stem/Stromal Cells Derived during Processing of Umbilical Cord Tissue. Cell Transplantation. 2018; 27: 181–193. https://doi.org/10.1177/0963689717744787.
[50] Vedicherla S, Buckley CT. Rapid Chondrocyte Isolation for Tissue Engineering Applications: The Effect of Enzyme Concentration and Temporal Exposure on the Matrix Forming Capacity of Nasal Derived Chondrocytes. BioMed Research International. 2017; 2017: 2395138. https://doi.org/10.1155/2017/2395138.
[51] Vedicherla S, Romanazzo S, Kelly DJ, Buckley CT, Moran CJ. Chondrocyte-based intraoperative processing strategies for the biological augmentation of a polyurethane meniscus replacement. Connective Tissue Research. 2018; 59: 381–392. https://doi.org/10.1080/03008207.2017.1402892.
[52] Raposio E, Caruana G, Bonomini S, Libondi G. A novel and effective strategy for the isolation of adipose-derived stem cells: minimally manipulated adipose-derived stem cells for more rapid and safe stem cell therapy. Plastic and Reconstructive Surgery. 2014; 133: 1406–1409. https://doi.org/10.1097/PRS.0000000000000170.
[53] Hunziker EB, Quinn TM, Häuselmann HJ. Quantitative structural organization of normal adult human articular cartilage. Osteoarthritis and Cartilage/OARS, Osteoarthritis Research Society. 2002; 10: 564–572. https://doi.org/10.1053/joca.2002.0814.
[54] Jurgens WJ, Kroeze RJ, Zandieh-Doulabi B, van Dijk A, Renders GA, Smit TH, *et al*. One-step surgical procedure for the treatment of osteochondral defects with adipose-derived stem cells in a caprine knee defect: a pilot study. BioResearch Open Access. 2013; 2: 315–325. https://doi.org/10.1089/biores.2013.0024.
[55] Steadman JR, Rodkey WG, Briggs KK, Rodrigo JJ. The microfracture technic in the management of complete cartilage defects in the knee joint. Der Orthopäde. 1999; 28: 26–32. https://doi.org/10.1007/s001320050318.
[56] Kreuz PC, Steinwachs MR, Erggelet C, Krause SJ, Konrad G, Uhl M, *et al*. Results after microfracture of full-thickness chondral de-

fects in different compartments in the knee. Osteoarthritis and Cartilage/OARS, Osteoarthritis Research Society. 2006; 14: 1119–1125. https://doi.org/10.1016/j.joca.2006.05.003.

[57] Salzmann GM, Sah B, Südkamp NP, Niemeyer P. Reoperative characteristics after microfracture of knee cartilage lesions in 454 patients. Knee Surgery, Sports Traumatology, Arthroscopy: Official Journal of the ESSKA. 2013; 21: 365–371. https://doi.org/10.1007/s00167-012-1973-y.

[58] Lu XL, Mow VC. Biomechanics of articular cartilage and determination of material properties. Medicine and Science in Sports and Exercise. 2008; 40: 193–199. https://doi.org/10.1249/mss.0b013e31815cb1fc.

[59] Roobrouck VD, Ulloa-Montoya F, Verfaillie CM. Self-renewal and differentiation capacity of young and aged stem cells. Experimental Cell Research. 2008; 314: 1937–1944. https://doi.org/10.1016/j.yexcr.2008.03.006.

[60] Asumda FZ, Chase PB. Age-related changes in rat bone-marrow mesenchymal stem cell plasticity. BMC Cell Biology. 2011; 12: 44. https://doi.org/10.1186/1471-2121-12-44.

[61] Stolzing A, Jones E, Mcgonagle D, Scutt A. Age-related changes in human bone marrow-derived mesenchymal stem cells: consequences for cell therapies. Mechanisms of Ageing and Development. 2008; 129: 163–173. https://doi.org/10.1016/j.mad.2007.12.002.

Editor's note: The Scientific Editor responsible for this paper was Xiaolei Zhang.

Received: 9th September 2024; **Accepted**: 19th December 2024; **Published**: 24th April 2025